Virchows Arch (2011) 458:281–290
DOI 10.1007/s00428-010-1023-4

ORIGINAL ARTICLE

The many faces of atypical Ewing's sarcoma. A true entity mimicking sarcomas, carcinomas and lymphomas

Isidro Machado · Rosa Noguera · Eduardo Alcaraz Mateos · Silvia Calabuig-Fariñas · F. Ignacio Aranda López · Antonio Martínez · Samuel Navarro · Antonio Llombart-Bosch

Received: 14 September 2010 / Revised: 3 November 2010 / Accepted: 30 November 2010 / Published online: 23 December 2010

Abstract Ewing's sarcoma family of tumours (ESFT) comprises a group of small round cell tumours (SRCT) genetically defined by specific chromosomal translocations resulting in a fusion of the *EWSR1* gene with a member of the ETS family of transcription factors. Atypical ESFT are the most challenging of the ESFT subtypes, and the differential diagnosis with other SRCT of bone and soft tissue is difficult since these subtypes can resemble other neoplasms. The present article describes nine cases of genetically confirmed, atypical ESFT, having unusual alterations at morphological and immunohistochemical (IHC) levels associated with atypical clinical presentation mimicking sarcomas, carcinomas and lymphomas. Present results demonstrate that ESFT showing overlapping morphological and immunohistochemical features with other SRCT of soft tissue and bone, or even with carcinomas or lymphoma, can be differentiated using molecular techniques. In SRCT with *EWSR1* translocation demonstrated by FISH, the RT-PCR analysis of specific sarcoma-related gene fusion can offer important clues for the diagnosis of specific entities, especially in tumours with unusual histopathology and/or IHC findings. Thus, we confirm that the integration of clinical, histopathological, IHC and genetic data becomes decisive in the diagnosis of bone and soft tissue sarcomas.

Keywords Atypical ESFT · Differential diagnosis

This study was performed with grants from the European Union (EuroBonet Project, contract no.: 018814) and RD06/0020/0102 Instituto de Salud Carlos III, Madrid.

I. Machado · R. Noguera · S. Calabuig-Fariñas · S. Navarro · A. Llombart-Bosch (✉)
Pathology Department, Medical School, Valencia University, Avda Blasco Ibáñez, 15, Valencia 46010, Spain
e-mail: antonio.llombart@uv.es

E. A. Mateos · F. I. A. López
Pathology Department, General Hospital Alicante, Alicante, Spain

A. Martínez
Pathology Department, General Hospital Torrevieja, Torrevieja, Spain

Introduction

Ewing's sarcoma family of tumours (ESFT) comprises a group of small round cell tumours (SRCT) mainly affecting the bone and soft tissues of children and young adults [12, 16–18, 20, 37]. ESFT are genetically defined by specific chromosomal translocations resulting in a fusion of the *EWSR1* gene with a member of the ETS family of transcription factors: *FLI1* (11q24), *ERG* (21q22), *FEV* (2q33), *ETV1* (7p22) and *ETV4* (17q12). In addition, other, less frequent, gene fusions have been described in ESFT, including *FUS/ERG*, *FUS/FEV*, *EWSR1/POU5F1*, *EWSR1/PATZ1*, *EWSR1/SP3*, *EWSR1/NFATc2*, *BRD4/NUT* and *CIC/DUX4* [3, 7, 20, 24, 32, 35].

The histopathology fluctuates between undifferentiated tumours (Ewing's sarcoma (ES)) and tumours with neuroectodermal differentiation/rosette formation (PNET) [12, 17, 18, 20, 32, 37]. Additionally, several histological varieties of ESFT are considered, including large cell ES, ES with epithelioid cells, clear cells, ES with spindle cells, vascular-like ES with haemangioendothelial features, ES with neuroectodermal features (isolated pseudorosettes), synovial sarcoma-like PNET, sclerosing PNET and adamantinoma-like ES [12, 17, 18, 20, 27, 32, 37]. In order to homogenize these ESFT subtypes, the tumours have been regrouped into three larger categories according

to their predominant morphological criteria: conventional/classical/typical ES, PNET with neuroectodermal features and atypical ES comprising all subtypes distinct from the other two types [12, 20].

Atypical ESFT are the most challenging of this group of tumours, and the differential diagnosis with other SRCT of bone and soft tissue is difficult since these subtypes can resemble other neoplasms [12, 17, 18, 20, 21, 27]. The present article describes nine cases of genetically confirmed, atypical ESFT presenting unusual structural findings at morphological and immunohistochemical (IHC) levels associated with conventional or more uncommon clinical presentations. These characteristics may complicate the differential diagnosis with other sarcomas, carcinomas and lymphomas, thus creating problems in formulating the therapeutic approach.

Clinical data

Age, gender and tumour location, histopathology findings, immunohistochemical, differential diagnosis and genetic results are summarized in Table 1.

Material and methods

The whole tumour specimen was fixed in buffered formalin, embedded in paraffin and processed for pathological investigation. Sections, 4 μm thick, were cut for haematoxylin/eosin (H/E), IHC and fluorescence in situ hybridization (FISH) studies. The antibodies employed, with their source and dilution, are summarized in Table 2. The immunostaining score was classified as non-informative (scant material, artefact and tumour necrosis), negative (mild in <5%), 1+ (mild in 5–10%), 2+ (moderate in 10–50%) and 3+ (intense in >50%). Positive nuclear staining was considered for Fli-1, myogenin and INI1 and cytoplasm/membranous staining was considered for CD99, CAV-1, HNK-1, osteonectin, osteocalcin, LCA, CD20, CD3, CD138, CK (AE1/AE3), CK20, EMA, SMA, desmin, synaptophysin, chromogranin, NB84, TH, HMB-45, Melan-a and CD117. *EWSR1* (22q12) (Vysis) and LSI *SYT* (18q11.2) (Vysis) break apart probes were used for FISH analysis. FISH was performed according to the conventional protocol for paraffin-embedded tumours in whole sections [24, 31, 34]. In normal cells two fused or very close (red-green) signals were observed. In cells with translocations, two types of signals were observed: one fused (red-green) signal, and another signal split into green and red. An average of 200 well-separated nuclei was counted in each case. A positive result was defined as more than 15% of cells with translocation. For RT-PCR analysis, total RNA was extracted using conventional protocols [24, 26]. The primer sets (Table 3) were applied according to the incidence of typical gene fusions for specific SRCT.

Results

Case 1 The histopathology revealed the presence of mature cortical and trabecular bone tissue, as well as soft tissue infiltrated by a malignant neoplasia of small round cells. The cytoplasm was abundant, slightly eosinophilic and occasionally vacuolate. Cells were distributed in strands, nests and small sheets within a richly vascularized, fibrohyaline stroma, and with perivascular deposits of a mantle of fibrillar, hyaline eosinophilic material, interposed among the neoplastic cells corresponding to reactive osteoid formation probably secondary to bone destruction (Fig. 1a, b). IHC study revealed positivity for CD99+++, FLi-1+++, HNK-1++,CAV-1+++, osteonectin+ (Fig. 1c), CK+++, EMA++ and INI1++. The tumour was negative for other markers including S-100, HMB-45, CD45, CD20, SMA and desmin. FISH analysis revealed a positive *EWSR1* break apart, and with RT-PCR an *EWSR1/Fli-1* fusion was demonstrated. The final diagnosis was atypical ESFT mimicking small cell osteosarcoma.

Case 2 Histopathologic studies revealed a proliferation of small round cell cells with scant eosinophilic cytoplasm and ill-defined cell borders, oval to round nuclei and moderate mitotic index. The cells were distributed in nests or strands embedded in a high desmoplastic stroma (Fig. 1d, e). Occasionally, pseudorosette structures were observed. The IHC showed strongly immunoreactive for CD99, Fli-1, CAV-1 (Fig. 1f) and CK (dot-like), moderately positive for HNK-1 and stained weakly for S100. EMA, desmin and SMA were negative. FISH analysis revealed *EWSR1* break apart positive and RT-PCR detected *EWSR1/Fll-1* gene fusion. The final diagnosis was atypical ESFT with desmoplasia, and the differential diagnosis was desmoplastic small round cell tumour (DSRCT).

Case 3 The histopathology showed the presence of a small cell tumour associated with prominent spindle cells proliferation (Fig. 1g, h). The cytoplasm was scant and slightly eosinophilic. Neither rosette formation nor glandular structures were detected. IHC study revealed positivity for CD99+++ (Fig. 1i), Fli-1+++, HNK-1++, CAV-1+++, CK+++ and EMA+. The tumour was negative for other markers including S-100, SMA and desmin. FISH analysis revealed a positive *EWSR1* break apart and negative *SYT*

Table 1 Clinicopathologic and genetic characteristics of the present series

Case	Age	Sex	Tumor location	Histopathology findings	Differential diagnosis	IHC results	FISH / RT-PCR
1	19	M	right Iliac bone	SRCT with reactive osteoid formation	Atypical ESFT vs SCO	CD99+,HNK1+,CAV1+, CK+,EMA+,Ost+	*EWSR1+EWS/Fli-1+*
2	29	M	retroperitoneal area	SRCT with desmoplasic stroma	Atypical ESFT vs DSRCT	CD99+,HNK1+,Fli1+, CAV1+,CK+,EMA-, Desmin-.	*EWSR1+EWS/Fli-1+*
3	15	M	Subscapular soft tissue	SRCT with spindle cells	Atypical ESFT vs Synovial sarcoma	CD99+,HNK1+,Fli1+, CAV1+,CK+,EMA-, Desmin-.	*EWSR1+EWS/ERG+*
4	28	M	Right inguinal area	SRCT with rhabdoid cells	Atypical ESFT vs rhabdomyosarcoma	CD99+,HNK1+,Fli1+, CAV1+,CK+,EMA-, Desmin-. Myogenin-, INI1+	*EWSR1+EWS/Fli-1+*
5	65	F	Right leg, soft tissue location	SRCT with prominent vascular formation	Atypical ESFT vs others soft tissus tumor with hemangioendothelial pattern.	CD99+,HNK1+,Fli1+, CAV1+,CK+,EMA-, Desmin-.Myogenin-,	*EWSR1+EWS/Fli-1+*
6	2	F	Paraverterbral area	SRCT without pseudorosette formation	Atypical ESFT vs neuroblastoma	CD99+,HNK1+,Fli1+, CAV1+,CK+,EMA-, Desmin-,NB84-,TH-.	*EWSR1+MYCN-EWS/Fli-1+*
7	33	F	Back region soft tissue	SRCT with seuglandular formation and desmoplasia	Atypical ESFT adamantinoma-like vs Myoepithelial carcinoma	CD99+,HNK1+,Fli1+, CAV1+,CK-,EMA+, Desmin-,S100-, SMA -.	*EWSR1+EWS/FEV+*
8	38	M	Right arm (superficial location)	SRCT with superficial location	Atypical ESFT vs Merkel carcinoma	CD99+,HNK1+,Fli1+, CAV1+,CK-,CK20-, EMA-,Desmin-,S100-, SMA -.	*EWSR1+EWS/Fli-1+*
9	85	M	Sacral area	SRCT with discohesive cells and previous history of NHL	Atypical ESFT vs NHL	CD99+,HNK1+,Fli1+, CAV1+,CK-,EMA-, Desmin-,S100-, SMA -, CD45-,CD20-,CD138-.	*EWSR1+EWS/Fli-1+*

translocation and the RT-PCR detected *EWSR1/ERG* gene fusion. The final diagnosis was atypical ESFT with spindle cell proliferation mimicking synovial sarcoma.

Case 4 The histopathology revealed the presence of soft tissue infiltrated by a malignant neoplasm of small round cells. The cytoplasm was prominent, eosinophilic with rhabdoid and rhabdomyoblast morphology (Fig. 2a, b). Cells were distributed in large sheets within a richly vascularized stroma. IHC study revealed positivity for CD99+++, Fli-1+++, HNK-1+++, CAV-1+++ (Fig. 2c), CK+++ and INI1++. The tumour was negative for EMA, SMA, desmin and myogenin. FISH analysis revealed a positive *EWSR1* break apart and RT-PCR detected *EWSR1/FLi-1* fusion, although *PAX/FKHR* fusion genes were not demonstrated. The final diagnosis was atypical ESFT with rhabdoid cells resembling adult pleomorphic rhabdomyosarcoma or malignant tumour with rhabdoid phenotype.

Case 5 The neoplasm showed an SRCT morphology, but with prominent vascular formation adopting a haemangioendothelial pattern (Fig. 2d, e). The tumour cell cytoplasm was scant and focal spindle cell morphology was observed. Neither rosette nor pseudorosette formation was detected. IHC study revealed positivity for CD99 (+++) (Fig. 2f), Fli-1 (+++), CAV1 (+++), HNK-1 (+) and CK. EMA, desmin, myogenin, SMA, S100, chromogranin and synaptophysin were negative. FISH analysis revealed positive translocation (break apart) for *EWSR1* gene and negative results for *SYT*. RT-PCR showed the *EWSR1/FEV* fusion transcript. No other gene fusions involved in specific SRCT (synovial sarcoma, extraskeletal myxoid chondrosarcoma, round/myxoid liposarcoma, DSRCT, clear cell sarcoma) were detected. The final diagnosis was atypical vascular ESFT resembling soft tissue tumour with vascular formation.

Table 2 Immunohistochemical study. Antibodies, source and dilution

Antibody	Source	Dilution
CD99	Dako	1:50
Caveolin-1	Santa Cruz	1:200
HNK-1	Valencia	no
Fli1	Santa Cruz	1:50
Osteonectin	Novoc ep	1:50
Osteocalcin	Chemicon	1:50
LCA	Dako	1:50
CD20	Dako	1:100
CD3	Dako	1:100
CD138	Santa Cruz	1:100
CK (AE1/AE3)	Dako	1:50
CK20	Dako	1:50
EMA	Dako	1:200
SMA	Novocastra	1:200
Desmin	Dako	1:100
Myogenin	Santa Cruz	1:50
Synaptophysin	Novoc	1:50
Cromogranin	Dako	1:50
NB84	Novoc	1:100
TH	Novoc ep	1:30
HMB-45	Novoc	1:50
MELAN-A	Dako	1:50
CD117	Dako	1:50
INI-1	BD	1:50

Case 6 Histopathologic studies revealed a proliferation of small round cell with scant cytoplasm and undifferentiated morphology, abundant apoptotic cells were observed and the mitotic index was low (Fig. 2g–i). Occasionally, pseudorosette structures were observed. The IHC showed positivity for CD99 (+++), FLI-1 (+++), CAV-1 (++), HNK-1 (+) and CK (+). EMA, desmin, SMA, NB84, TH, CD45, CD20, chromogranin and synaptophysin were negative. FISH analysis revealed *EWSR1* break apart positive and no *MYCN* gene amplification. RT-PCR detected *EWSR1/Fli-1* gene fusion. The final diagnosis was atypical ESFT (large cells) mimicking undifferentiated neuroblastoma.

Case 7 The neoplasm showed and SRCT morphology. The cytoplasm fluctuated from scant to abundant and clear or eosinophilic appearance was observed. Tumour cells were arranged in several patterns including diffuse SRCT, tubular, cord-like, clear cells, epithelioid and pseudo-glandular. In several areas the tumour cells adopted a palisading architecture, being sustained by a collagen basal-like membrane (Fig. 3a, b). This basement membrane was homogeneous, eosinophilic and PAS positive. IHC study revealed positivity for CD99 (+++) (Fig. 3c), Fli1(+++), CAV1 (+++) and HNK-1 (++). Poor cytoplasmic expression for EMA was observed. CK, desmin, SMA, S100 and myogenin were negative. FISH analysis revealed positive translocation (break apart) for *EWSR1* gene and negative results for *SYT*. RT-PCR showed the *EWSR1/FEV* fusion transcript. No other gene fusions involved in specific SRCT (synovial sarcoma, extraskeletal myxoid chondrosarcoma, round/myxoid liposar-

Table 3 Primers used for RT-PCR

Primers	DNA sequence
EWS7ARF	TCCTACAGCCAAGCTCCAAGTCAATA
EWS8.1RF	GCATGAGTGGCCCTGATAAC
EWS9DRF	CTGGTGGACCCATGGATGAAGGA
EWS10GRF	TGGAGAGCGAGGTGGCTTCAATAA
EWS11RF	TCTGGCAGACTTCTTTAAGCA
FLI6ARR	ATTGCCCCAAGCTCCTCTTCTGAC
FLI5BRR	TCGGTGTGGGAGGTTGTATT
EWS7ARF	TCCTACAGCCAAGCTCCAAGTCAATA
ERG6ERR	CTCCTGGGGGGCTCATATGGTAAAT
ERG9KRR	TGAGGGGTACTTGTACAGA
EWS7ARF	TCCTACAGCCAAGCTCCAAGTCAATA
FEV11	TGTTGGGCTTGCTCTTGCGCTC
FEVF1RR	GCTTGAACTCGCCGTGACCG
EWS7ARF	TCCTACAGCCAAGCTCCAAGTCAATA
ETV6-RF	GCTTACATGAACCACATCATGG
EWS22.3RF	TCCTACAGCCAAGCTCCAAGTC
ATF1-RR1	GAAGTCCCTGTACTCCATCTGTG
EWS22.3RF	TCCTACAGCCAAGCTCCAAGTC
WT1-9RR	GACCAGGAGAACTTTCGCTGAC
WT1-8RR	ACCTTCGTTCACAGTCCTTG
WT1-10RR	GCCACCGACAGCTGAAGGGC
SSX1RR	GGTGCAGTTGTTTCCCATCG
SSX2RR	GGCACAGCTCTTTCCCATCA
SYTRF	CAACAGCAAGATGCATACCA
MGBRF	CTCGCGCTACTCTCTCTTTCT
MGBRR	TGTCGGATTGATGAAACCCAG
EWS12BRF	GCGATGCCACAGTGGCCTATG
CHN2RR	GGACGTCCGGCGAGGCGAAGC
CHN3RR	CCTGGAGGGGAAGGGCTAT
PAX3/7-1	CCGACAGCAGCTCTGCCTAC
PAX3U	CCAAACACAGCATCGACG
PAX7U	TTTGAGAGGACCCACTACCC
FKHR-2	ATGAACTTGCTGTGTAGGGACAG
ETV6-RF	GCTTACATGAACCACATCATGG
NTRK3-RR	GAAGTCGTGCTACAGAGAGG

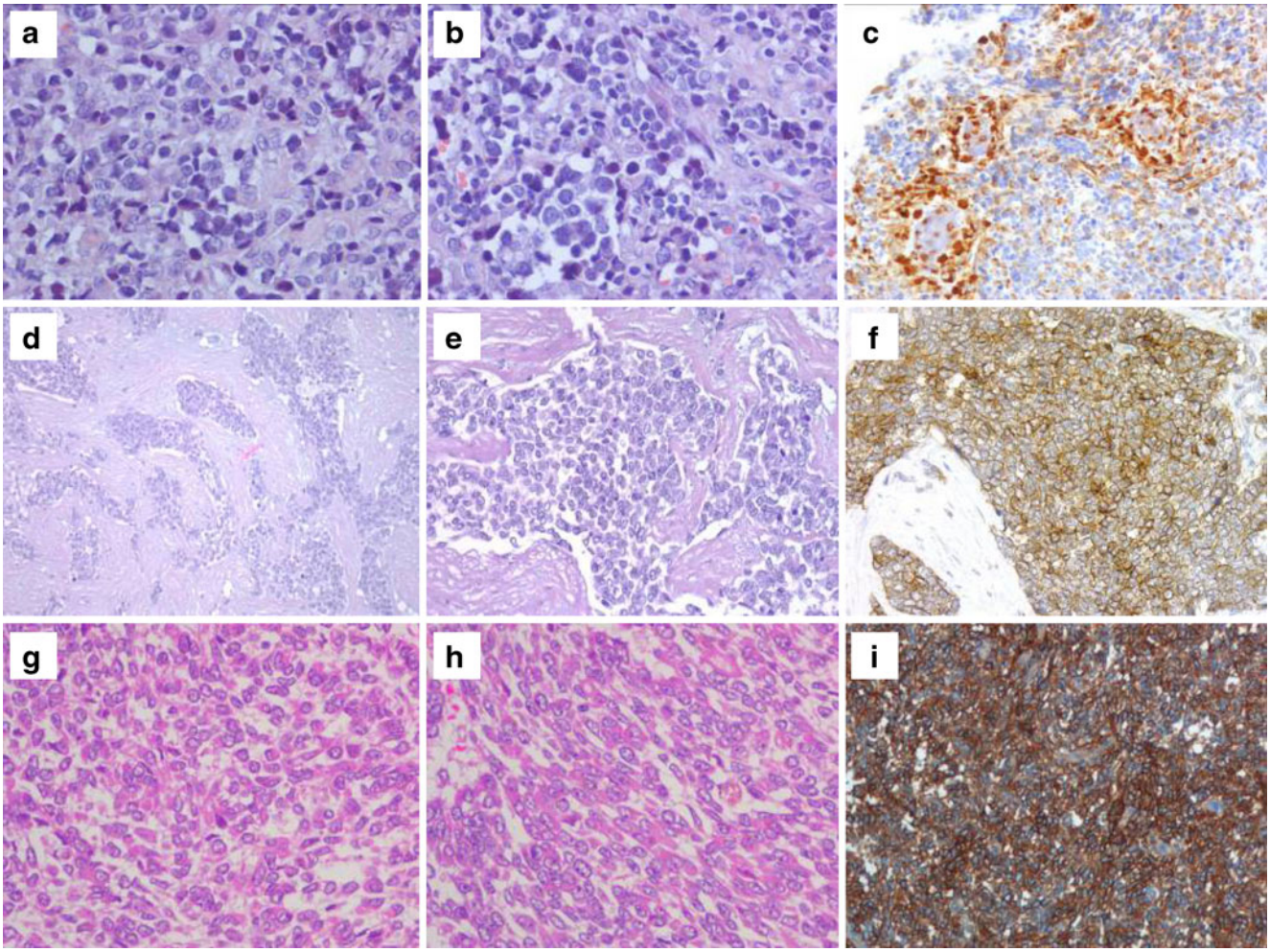

Fig. 1 **a** Case 1, atypical ESFT with hyaline eosinophilic material, interposed among the neoplastic cells [haematoxylin and eosin (H&E ×40)]. **b** Case 1, atypical large cell ESFT (H&E ×40). **c** Case 1, osteonectin cytoplasmic staining (+++) in reactive bone and poor positivity in ESFT neoplastic cells. **d** Case 2, atypical ESFT with extensive desmoplastic stroma (H&E ×20). **e** Case 2, atypical ESFT with cells distributed in nests or strands embedded in a highly desmoplastic stroma (H&E ×40). **f** Case 2, caveolin-1 membranous staining (+++) in neoplastic cells. **g** Case 3, atypical ESFT with small cell tumour showing slightly eosinophilic cytoplasm (H&E ×40), **h** case 3, atypical ESFT associated with prominent spindle cell proliferation (H&E ×40). **i** Case 3, CD99 membranous staining (+++) in tumour cells

coma, DSRCT or clear cell sarcoma) were detected. The final diagnosis was atypical ESFT (adamantinoma-like) resembling soft tissue myoepithelial carcinoma.

Case 8 The round cell neoplasm was restricted to the dermis (Fig. 3d, e). The tumour was composed of sheets and lobules of small- to medium-sized round cells showing scant cytoplasm. Mitotic index was low and neither necrosis nor pseudorosette formation were observed. IHC study revealed positivity for CD99 (+++) (Fig. 3f), Fli1 (++), CAV1 (++) and HNK-1 (+). CK, CK20, EMA, desmin, SMA, S100 and myogenin were negative. FISH analysis revealed positive translocation for *EWSR1* gene and RT-PCR showed the *EWSR1/Fli-1* fusion transcript. No other gene fusions involved in specific SRCT (synovial sarcoma, extraskeletal myxoid chondrosarcoma, round/myxoid liposarcoma, DSRCT or clear cell sarcoma) were detected. The final diagnosis was atypical superficial ESFT mimicking Merkel cell carcinoma.

Case 9 Histopathologic studies revealed a proliferation of small round cell cells with very incohesive cells and no intervening stroma mimicking lymphoma neoplasm (Fig. 3g, h). The cells showed scant cytoplasm and the mitotic index was low. No pseudorosette structures were observed. The IHC showed positivity for CD99, FLI-1, CAV-1 and HNK-1. CK, EMA, desmin, CD45, CD20, CD3 and CD138 were negative. FISH analysis revealed *EWSR1* break apart positivity (Fig. 3i) and RT-

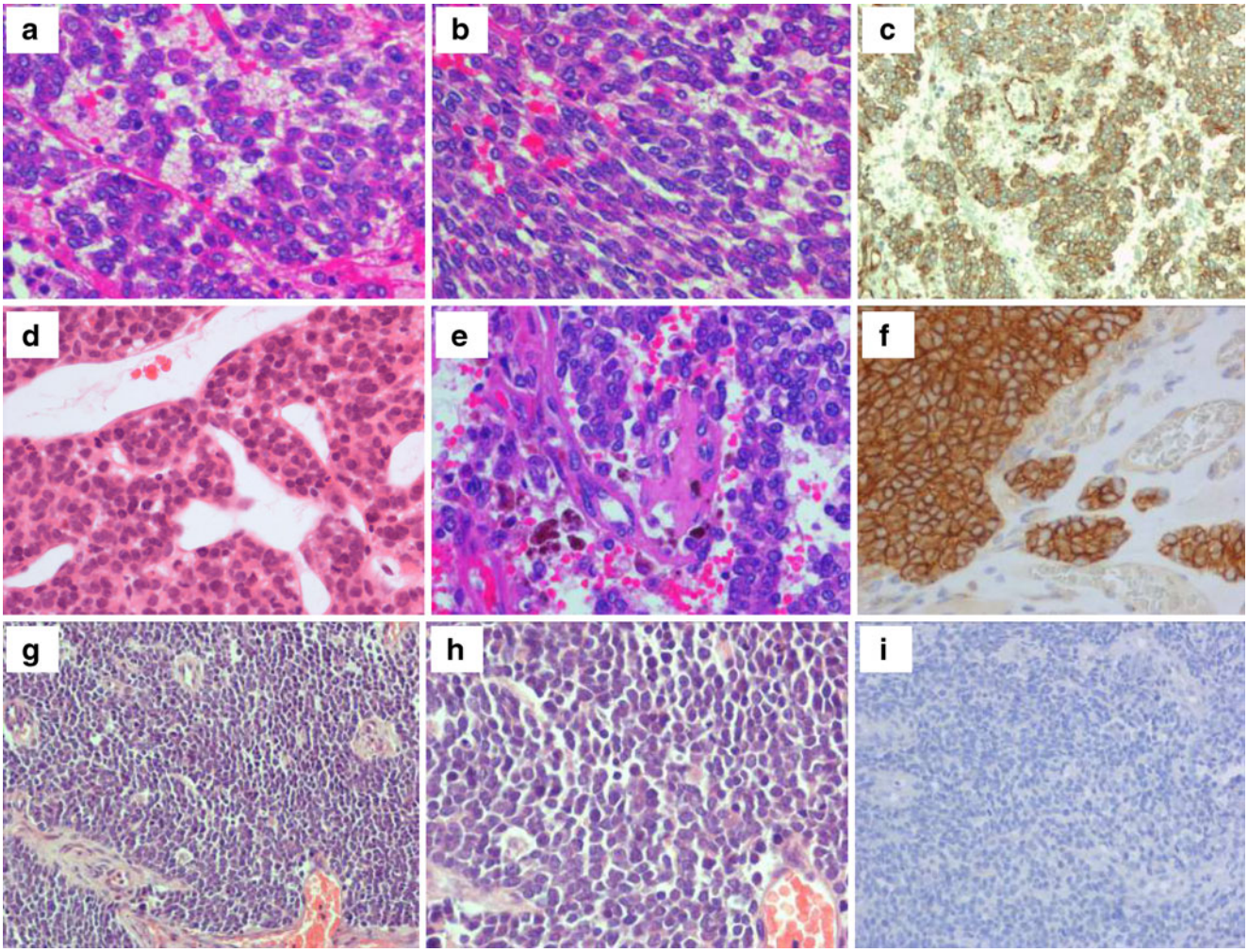

Fig. 2 **a** Case 4, atypical ESFT with prominent eosinophilic cytoplasm (H&E ×40). **b** Case 4, atypical ESFT, the cytoplasm showing rhabdoid and rhabdomyoblast morphology (H&E ×40). **c** Case 4, caveolin-1 cytoplasmic staining (+++) in tumour cells. **d** Case 5, atypical ESFT with prominent vascular formation (H&E ×40). **e** Case 5, atypical ESFT with haemosiderin deposition and vascular formation (H&E ×40). **f** Case 5, CD99 membranous staining (+++). **g** Case 6, atypical ESFT with undifferentiated morphology (H&E ×20). **h** Case 6, atypical ESFT, scant cytoplasm, undifferentiated morphology and vascular formation (H&E ×40). **i** Case 6, atypical ESFT, negative for NB84

PCR detected an *EWSR1/Fli-1* gene fusion. The final diagnosis was atypical ESFT resembling non-Hodgkin lymphoma (patient with previous history of non-Hodgkin lymphoma).

Discussion

Atypical variants of ESFT have been described mostly by Nascimiento et al. [27], Llombart-Bosch et al. [17, 18, 20] and Folpe et al. [12]. The criteria used for these histological subtypes include the high degree of cell heterogeneity, the existence of unusual patterns or the presence of pseudovascular structures [12, 20]. Cell heterogeneity of atypical ESFT is consistent with the presence of large, clear, spindle, epithelioid or rhabdoid cells in wide areas of the tumour [12, 20, 27]. The existence of unusual patterns is characterized by components such as desmoplasia, sclerosis and adamantinoma-like areas [6, 12, 13, 20, 27, 37]. Pseudovascular structures offer in atypical ESFT a vascular-like haemangiomatous appearance [20]. In these cases, the correlation between the clinical data (tumour location, age and sex), morphological, IHC and genetic findings is mandatory [12, 20]. Additionally, epithelial differentiation has been demonstrated in 20% of genetically confirmed ESFT [15]. Particularly, the atypical variant of ESFT frequently shows epithelial differentiation at histological and IHC level, further complicating the differential diagnosis with other SRCT of bone and soft tissue with CK immunoexpression (adamantinoma, synovial sarcoma, rhabdomyosarcoma, epithelioid sarcoma, DSRCT, malignant rhabdoid tumour (MRT) or tumour with rhabdoid

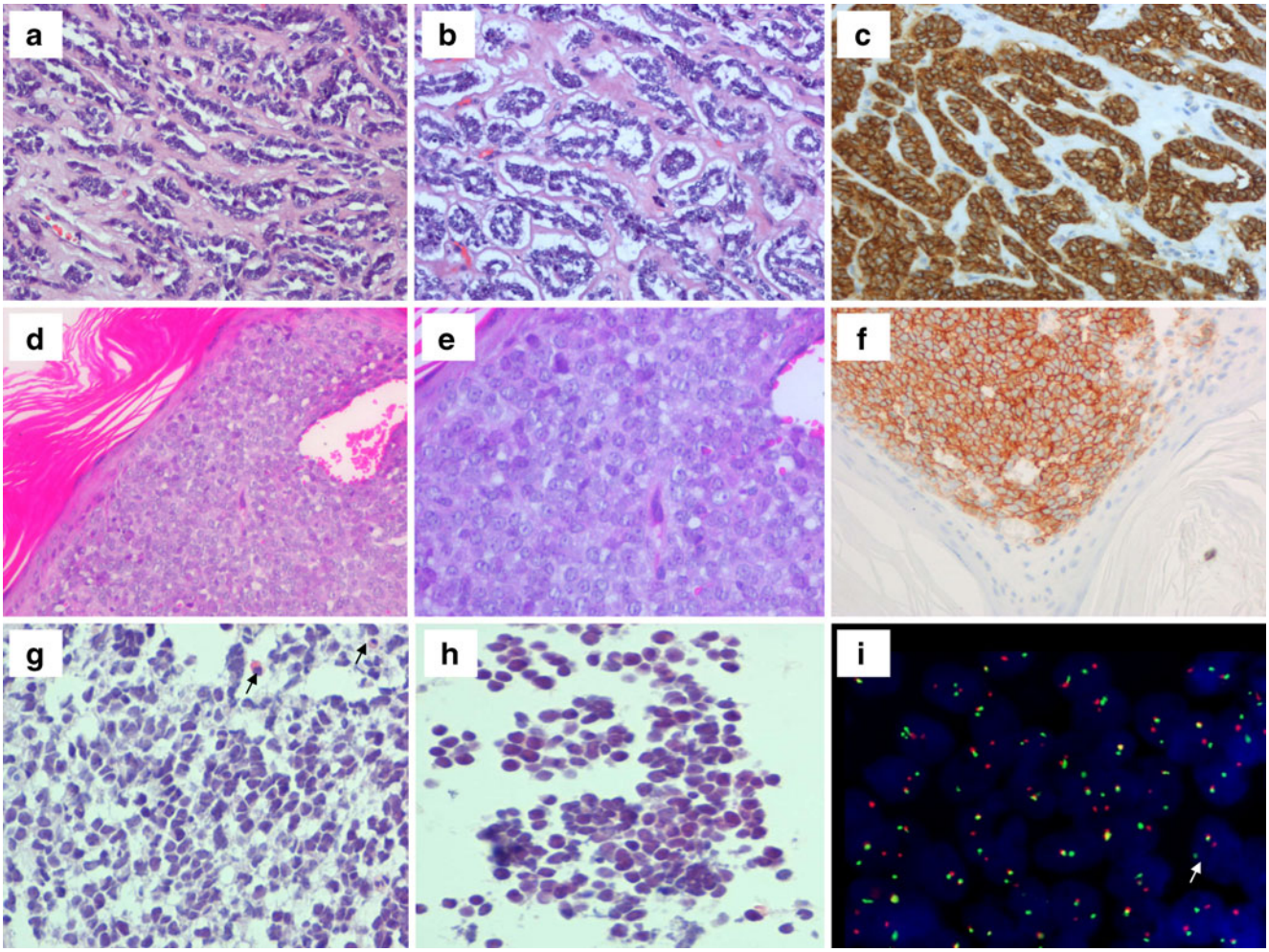

Fig. 3 **a** Case 7, atypical ESFT with adamantinoma-like structures (H&E ×40). **b** Case 7, atypical ESFT, cord-like, clear cells, epithelioid and pseudo-glandular patterns. The tumour cells adopted a palisading architecture, being sustained by a collagen basal-like membrane (H&E ×40). **c** Case 7, CD99 membranous and cytoplasmic staining (+++) in tumour cells. **d** Case 8, atypical cutaneous ESFT with neoplastic cells restricted to the dermis (H&E ×20). **e** Case 8, superficial atypical ESFT (H&E ×40). **f** Case 8, CD99 membranous staining (+++) in tumour cells and negative in cutaneous epithelial structures. **g** Case 9, atypical ESFT with undifferentiated morphology, and scant eosinophilic and plasma cells (*arrow*; H&E ×40). **h** Case 9, atypical ESFT, incohesive cells and undifferentiated morphology mimicking lymphoblastic lymphoma (H&E ×40). **i** Case 9, atypical ESFT, FISH/*EWSR1* with break apart (*arrows*), positive for *EWSR1* translocation

phenotype, myoepithelial carcinoma, neuroendocrine carcinomas and metastatic carcinomas). Furthermore, many of these soft tissue tumours (DSRCT, myoepithelial carcinoma and neuroendocrine carcinoma) can display an *EWSR1* rearrangement by fluorescence in situ hybridization which complicates the differential diagnosis with atypical ESFT [4, 5, 25, 29]. Therefore, the use of RT-PCR analysis to detect specific gene fusions in the latter cases is mandatory.

In the present series, we describe nine cases of SRCT with a genetically confirmed final diagnosis of atypical ESFT, resembling sarcomas, carcinomas and lymphomas due to the presence of unusual cell morphology or atypical patterns. Six cases (1–6) mimic sarcomas with or without osteoid formation. Age and tumour location in (case 1) were concordant with the diagnosis of ESFT; however, osteoid deposition and EMA IHC positivity were unexpected characteristics. The osteoid deposits complicated the differential diagnosis with small cell osteosarcoma (SCO); and the EMA positivity with undifferentiated synovial sarcoma. Molecular studies revealing *EWSR1* translocation and *EWSR1/Fli1* gene fusion, a finding inconsistent with synovial sarcoma, defined the diagnosis of atypical ESFT in case 1. It seems reasonable that in any atypical SRCT with osteoid deposition, CD99 positivity and *EWSR1* rearrangement, the confirmation of the translocation should be carried out by two different molecular methods. On the other hand, ESFT can reveal osteoid deposition and IHC osteonectin positivity due to reactive new bone formation. Moreover, in cases with presumptive diagnosis of ESFT in bone, but negative for the specific translocations or gene

fusions, the possibility of SCO should be excluded and several histopathological sections from the paraffin block are mandatory to exclude malignant osteoid formation [2, 10, 23]. Definitively, despite the morphological link between ESFT and SCO, malignant osteoid formation remains the hallmark of SCO, while the presence of an *EWSR1* translocation with the specific gene fusions are diagnostic of ESFT [23]. Despite the CK and EMA positivity in the present tumour, the diagnosis of synovial sarcoma was excluded since molecular studies did not reveal *SYT* rearrangement. As far as we know, EMA expression has not so far been described in genetically confirmed ESFT, so this finding complicated the differential diagnosis with other SRCT with EMA expression (synovial sarcoma, MRT, epithelioid sarcoma and myoepithelial carcinoma). To our knowledge, loss of INI1 expression has not yet been reported in ESFT; however, this is a frequent event in MRT, and occasionally, epithelioid sarcoma, myoepithelial carcinoma, epithelioid malignant peripheral nerve sheath tumour and synovial sarcoma can reveal loss of INI1 expression.

Findings resembling DSRCT (desmoplastic stroma; case 2) are unusual in ESFT [12, 20, 37]. Nevertheless, an unusual subtype of ESFT with desmoplasia has been described by Folpe et al. [12]. In case 2, the retroperitoneal location, desmin negativity and *EWSR1/Fli1* gene fusion by RT-PCR are more consistent with ESFT than with DSRCT. However, DSRCT with *EWSR1/Fli1* or *EWSR1/ERG* gene fusion have already been described, but with evident IHC desmin expression [28]. Desmin expression is very rare in ESFT, nevertheless sporadic studies have reported this finding in which the tumours were classified as biphenotypic sarcomas with or without *EWSR1* rearrangement [9, 33]. Indeed, in desmin-positive SRCT, the possibility of ESFT remains very unlikely and the possibility of other SRCT with muscular differentiation (rhabdomyosarcoma and SCO) should be exhaustively excluded. Furthermore, in a recent study performed by Llombart-Bosch et al. in more than 500 genetically confirmed ESFT, desmin expression was absent in all tumours (data unpublished). The term 'biphenotypic sarcoma' has been used for tumours with either neural and muscular differentiation, or neural and osteoid production, although the actual existence of these tumours is still under debate. In fact, in the post-molecular era only very sporadic reports regarding biphenotypic sarcoma have been published, and the existence of this particular neoplasm is becoming doubtful.

A sarcoma without osteoid production and with predominant spindle cells expressing CK made the differential diagnosis between atypical ES and undifferentiated synovial sarcoma difficult (case 3). In this case, tumour location and age are suggestive of both tumours; however, EMA negativity and the absence of *SYT* translocation and S*YT/SSX* transcript made the existence of synovial sarcoma improbable [9, 11, 19]. Additionally, the finding of *EWSR1* translocation and *EWSR1/ERG* gene fusion confirms the diagnosis of ESFT, in this case atypical ESFT with spindle cells.

Tumour location (inguinal region), the morphologic characteristics of tumour cells (abundant eosinophilic cytoplasm) made the differential diagnosis between atypical ES and adult rhabdomyosarcoma difficult [11, 19, 30] (case 4). FISH analysis revealed *EWSR1* translocation and the RT-PCR, *EWSR1/Fli1* transcript confirmed the diagnosis of ESFT. In addition, desmin, myogenin and SMA were negative, making the possibility of adult rhabdomyosarcoma unlikely. Despite the age of the patient, the possibility of alveolar rhabdomyosarcoma was excluded since the RT-PCR failed to detect *PAX-FKHR* gene fusion.

In atypical ESFT, vascular-like areas have been reported similar to case 5 in which the tumour cells display a pseudoendothelial pattern forming vascular or lacunar spaces, lined by tumour cells that progressively elongate and cover lacunae filled with erythrocytes and plasma material [12, 18, 20]. Tumour cells, lining the surface of the vessel-like spaces lack basal membrane and are in continuity with the more solid cellular fields [12, 18, 20]. Abundant vascular formation with erythrocyte lysis can generate haemosiderin deposits, misinterpreted clinically as the melanic pigment observed in melanoma or clear cell sarcoma.

Tumour location (paravertebral area), patient age and absence of pseudorosette formation can make the differential diagnosis between neuroblastoma and atypical ESFT difficult (case 6). Children below 5 years of age with SRCT of bone and soft tissue should be carefully evaluated to exclude metastatic neuroblastoma [8, 31]. The present case showed IHC findings suggestive of ESFT instead of neuroblastoma, and additionally the *EWSR1* translocation was demonstrated by FISH and RT-PCR.

Differential diagnosis of atypical ESFT with carcinomas is quite complex in some tumours (cases 7 and 8). The soft tissue tumour location and the trabecular, tubular and pseudo-glandular patterns at histological level made the differential diagnosis with adamantinoma-like EFST and soft tissue myoepithelial carcinoma confusing [5, 14] (case 7). Myoepithelial carcinoma displays epithelial and neural differentiation with CK and S100 expression [5, 14] and both markers were negative in case 7, making the diagnosis of myoepithelial carcinoma improbable. The differential diagnosis has become more complex since Brandal et al. [5] described the *EWSR1* rearrangement in myoepithelial carcinomas with (*EWSR1/ZNF444*) gene fusion. Furthermore, Antonescu et al. [1] described the same finding in a large series of myoepithelial carcinomas. The finding of an *EWSR1/FEV* gene fusion is probably the principal event in this case, and it is unlikely that another gene fusion

involving *EWSR1* would be detected in the same tumour despite *EWSR1* translocation by FISH. On the other hand, due to the partial epithelial nature (EMA positive) of the present tumour, metastatic carcinoma should also be considered in the differential diagnosis, including neuroendocrine carcinoma that may harbour *EWSR1* translocation, as recently described [25]. This patient had no previous history of carcinoma and neuroendocrine markers were negative. Although the morphological features (cord-like, tubular epithelioid and pseudo-glandular patterns) were uncommon for ESFT, case 7 was finally diagnosed as adamantinoma-like ESFT.

The superficial location (dermis) of the tumour and round cell morphology complicated the differential diagnosis between atypical ES and Merkel cell carcinoma [22, 32, 36] (case 8). However, Merkel cell carcinoma usually displays CK20 expression, while the present case was negative for this marker. *EWSR1* translocation (FISH and RT-PCR) confirmed the diagnosis of superficial atypical ESFT. Nevertheless, ESFT can occur as a cutaneous tumour, making the differential diagnosis with Merkel cell tumours complex [22, 32, 36], especially when 20% of ESFT have epithelial differentiation (CK+) and in several cases Merkel cell neoplasms express CD99 [22, 32, 36]. Additionally, CK20 immunoreactivity is consistent with Merkel cell carcinoma, while its expression is absent in ESFT, as confirmed by our working group in more than 500 genetically confirmed ESFT tested with CK20 with lacking expression in all tumours (unpublished data).

Atypical ESFT can be confused with haematological disease [16–18], particularly in patients with a previous history of lymphomas (case 9). Lymphoid markers (CD45, CD20 and CD138) were negative in this case, thus excluding lymphoma/myeloma, and genetic studies revealed *EWSR1* translocation confirming the diagnosis of ESFT.

In conclusion, the cases herein reported represent unusual histological variants of ESFT mimicking sarcomas, carcinomas and lymphomas. These results strongly suggest that tumours showing overlapping morphological and immunohistochemical features with other SRCT of soft tissue and bone can be readily differentiated using complementary molecular techniques. In SRCT with an *EWSR1* translocation demonstrated by FISH, the RT-PCR analysis of specific sarcoma-related gene fusions can offer important clues when diagnosing specific entities, especially in tumours with atypical histopathology and/or IHC findings. However, for the time being the integration of clinical, histopathological, IHC and genetic data remains the corner stone for the diagnosis of bone and soft tissue sarcomas in which genetic rearrangements with reciprocal translocations are present.

Conflict of interest statement We declare that we have no conflict of interest.

References

1. Antonescu CR, Zhang L, Chang NE et al (2010) EWSR1-POU5F1 fusion in soft tissue myoepithelial tumors. A molecular analysis of 66 cases, including soft tissue, bone, and visceral lesions, showing common involvement of the EWSR1 gene. Genes Chromosom Cancer 49:1114–1124
2. Ayala AG, Ro JY, Papadopoulos NK et al (1993) Small cell osteosarcoma. Cancer Treat Res 62:139–149
3. Bovee JV, Hogendoorn PC (2010) Molecular pathology of sarcomas: concepts and clinical implications. Virchows Arch 456:193–199
4. Brandal P, Panagopoulos I, Bjerkehagen B et al (2008) Detection of a t(1;22)(q23;q12) translocation leading to an EWSR1-PBX1 fusion gene in a myoepithelioma. Genes Chromosom Cancer 47:558–564
5. Brandal P, Panagopoulos I, Bjerkehagen B et al (2009) t(19;22)(q13;q12) Translocation leading to the novel fusion gene EWSR1-ZNF444 in soft tissue myoepithelial carcinoma. Genes Chromosom Cancer 48:1051–1056
6. Bridge JA, Fidler ME, Neff JR et al (1999) Adamantinoma-like Ewing's sarcoma: genomic confirmation, phenotypic drift. Am J Surg Pathol 23:159–165
7. Bridge RS, Rajaram V, Dehner LP et al (2006) Molecular diagnosis of Ewing sarcoma/primitive neuroectodermal tumor in routinely processed tissue: a comparison of two FISH strategies and RT-PCR in malignant round cell tumors. Mod Pathol 19:1–8
8. Burgues O, Navarro S, Noguera R et al (2006) Prognostic value of the International Neuroblastoma Pathology Classification in Neuroblastoma (Schwannian stroma-poor) and comparison with other prognostic factors: a study of 182 cases from the Spanish Neuroblastoma Registry. Virchows Arch 449:410–420
9. de Alava E, Lozano MD, Sola I et al (1998) Molecular features in a biphenotypic small cell sarcoma with neuroectodermal and muscle differentiation. Hum Pathol 29:181–184
10. Devaney K, Vinh TN, Sweet DE (1993) Small cell osteosarcoma of bone: an immunohistochemical study with differential diagnostic considerations. Hum Pathol 24:1211–1225
11. Fisher C (2010) Soft tissue sarcomas with non-EWS translocations: molecular genetic features and pathologic and clinical correlations. Virchows Arch 456:153–166
12. Folpe AL, Goldblum JR, Rubin BP et al (2005) Morphologic and immunophenotypic diversity in Ewing family tumors: a study of 66 genetically confirmed cases. Am J Surg Pathol 29:1025–1033
13. Fukunaga M, Ushigome S (1998) Periosteal Ewing-like adamantinoma. Virchows Arch 433:385–389
14. Gleason BC, Fletcher CD (2007) Myoepithelial carcinoma of soft tissue in children: an aggressive neoplasm analyzed in a series of 29 cases. Am J Surg Pathol 31:1813–1824
15. Gu M, Antonescu CR, Guiter G et al (2000) Cytokeratin immunoreactivity in Ewing's sarcoma: prevalence in 50 cases confirmed by molecular diagnostic studies. Am J Surg Pathol 24:410–416
16. Li S, Siegal GP (2010) Small cell tumors of bone. Adv Anat Pathol 17:1–11
17. Llombart-Bosch A (1996) Small round cell tumors of bone and soft tissue. Introduction. Semin Diagn Pathol 13:149–152
18. Llombart-Bosch A, Contesso G, Peydro-Olaya A (1996) Histology, immunohistochemistry, and electron microscopy of small round cell tumors of bone. Semin Diagn Pathol 13:153–170
19. Llombart-Bosch A, Lopez-Guerrero JA, Peydro-Olaya A (2002) Synovial sarcoma (SS): new perspectives supported by modern technology. Arkh Patol 64:39–47

20. Llombart-Bosch A, Machado I, Navarro S et al (2009) Histological heterogeneity of Ewing's sarcoma/PNET: an immunohistochemical analysis of 415 genetically confirmed cases with clinical support. Virchows Arch 455:397–411
21. Llombart-Bosch A, Pellin A, Carda C et al (2000) Soft tissue Ewing sarcoma—peripheral primitive neuroectodermal tumor with atypical clear cell pattern shows a new type of EWS-FEV fusion transcript. Diagn Mol Pathol 9:137–144
22. Llombart B, Monteagudo C, Lopez-Guerrero JA et al (2005) Clinicopathological and immunohistochemical analysis of 20 cases of Merkel cell carcinoma in search of prognostic markers. Histopathology 46:622–634
23. Machado I, Alberghini M, Giner F et al (2010) Histopathological characterization of small cell osteosarcoma with immunohistochemistry and molecular genetic support. A study of 10 cases. Histopathology 57:162–167
24. Machado I, Noguera R, Pellin A et al (2009) Molecular diagnosis of Ewing sarcoma family of tumors: a comparative analysis of 560 cases with FISH and RT-PCR. Diagn Mol Pathol 18:189–199
25. Malone VS, Dobin SM, Jones KA et al (2010) CD99-positive large cell neuroendocrine carcinoma with rearranged EWSR1 gene in an infant: a case of prognostically favorable tumor. Virchows Arch 457:389–395
26. Mangham DC, Williams A, McMullan DJ et al (2006) Ewing's sarcoma of bone: the detection of specific transcripts in a large, consecutive series of formalin-fixed, decalcified, paraffin-embedded tissue samples using the reverse transcriptase-polymerase chain reaction. Histopathology 48:363–376
27. Nascimento AG, Unii KK, Pritchard DJ et al (1980) A clinicopathologic study of 20 cases of large-cell (atypical) Ewing's sarcoma of bone. Am J Surg Pathol 4:29–36
28. Ordi J, de Alava E, Torne A et al (1998) Intraabdominal desmoplastic small round cell tumor with EWS/ERG fusion transcript. Am J Surg Pathol 22:1026–1032
29. Ordonez NG (1998) Desmoplastic small round cell tumor: I: a histopathologic study of 39 cases with emphasis on unusual histological patterns. Am J Surg Pathol 22:1303–1313
30. Parham DM, Ellison DA (2006) Rhabdomyosarcomas in adults and children: an update. Arch Pathol Lab Med 130:1454–1465
31. Piqueras M, Navarro S, Castel V et al (2009) Analysis of biological prognostic factors using tissue microarrays in neuroblastic tumors. Pediatr Blood Cancer 52:209–214
32. Romeo S, Dei Tos AP (2010) Soft tissue tumors associated with EWSR1 translocation. Virchows Arch 456:219–234
33. Sorensen PH, Shimada H, Liu XF et al (1995) Biphenotypic sarcomas with myogenic and neural differentiation express the Ewing's sarcoma EWS/FLI1 fusion gene. Cancer Res 55:1385–1392
34. Subramaniam MM, Noguera R, Piqueras M et al (2007) Evaluation of genetic stability of the SYT gene rearrangement by break-apart FISH in primary and xenotransplanted synovial sarcomas. Cancer Genet Cytogenet 172:23–28
35. Szuhai K, Ijszenga M, de Jong D et al (2009) The NFATc2 gene is involved in a novel cloned translocation in a Ewing sarcoma variant that couples its function in immunology to oncology. Clin Cancer Res 15:2259–2268
36. Terrier-Lacombe MJ, Guillou L, Chibon F et al (2009) Superficial primitive Ewing's sarcoma: a clinicopathologic and molecular cytogenetic analysis of 14 cases. Mod Pathol 22:87–94
37. Ushigome U, Machinami R, Sorensen PH (2002) Ewing sarcoma/Primitive neuroectodermal tumor (PNET). In: Fletcher CDM, Unni K, Mertens F (eds) World health organization classification of tumours. Pathology and genetics of tumours of soft tissue and bone. IARC, Lyon